Bull. Mater. Sci. (2019) 42:73
https://doi.org/10.1007/s12034-019-1775-7

Poly(amido amine) dendrimer and silver nanoparticle–multi-walled carbon nanotubes composite with poly(neutral red)-modified electrode for the determination of ascorbic acid

C LAKSHMI DEVI and S SRIMAN NARAYANAN*
Department of Analytical Chemistry, School of Chemical Sciences, University of Madras, Guindy Campus, Chennai 600 025, Tamil Nadu, India
*Author for correspondence (sriman55@gmail.com)

MS received 6 June 2018; accepted 26 September 2018; published online 6 March 2019

Abstract. A new film containing poly(amido amine) dendrimer, silver nanoparticles and multi-walled carbon nanotubes composite with poly(neutral red) was prepared on a paraffin wax impregnated graphite electrode. The PAMAM/AgNPs–MWCNT/PNR film exhibited promising electrocatalytic oxidation of ascorbic acid (AA) in acetate buffer solution of pH 4.0. The PAMAM/AgNPs–MWCNT/PNR film-modified electrode enhanced the sensitivity of detection of AA. The PAMAM/AgNPs–MWCNT/PNR film-modified electrode was characterized by cyclic voltammetry, chronoamperometry, hydrodynamic voltammetry (HDV) and difference pulse voltammetry. These experiments confirmed the electrocatalytic oxidation of AA by PAMAM/AgNPs–MWCNT/PNR film-modified electrode. The PAMAM/AgNPs–MWCNT/PNR-modified electrode has been found to possess good electrocatalytic activity towards AA oxidation which has been observed at a lower oxidation potential of around 0.26 V with a higher current response. The electrochemical oxidation of AA by PAMAM/AgNPs–MWCNT/PNR-modified electrode involved a two proton and two electron process. A linear relationship between the catalytic current and AA concentration was obtained in the range from 0.16 to 2500 μM with a detection limit of 0.053 μM.

Keywords. Dendrimer; ascorbic acid; nanoparticles; electrocatalytic oxidation.

1. Introduction

Ascorbic acid (AA), known as vitamin C is a water-soluble anti-oxidant present in foods, drinks, citrus fruits, vegetables and leafy vegetables. It is also important in several human, animal and plant metabolic processes involving oxidation and reduction. AA is a medication for scurvy, drug poisoning, liver disease, allergic reactions, atherosclerosis and it helps to promote healthy cell development, calcium absorption and normal tissue growth [1]. It is used for the prevention and treatment of the common cold, mental illness, infertility, cancer and AIDS [2]. Therefore, the detection of AA is of great importance in pharmaceutical, clinical and the food industry [3,4]. Several methods are available for the determination of AA, such as chemiluminescence [5], chromatography [6], titrimetry [7], enzymatic analysis [8] and electrochemical methods [9]. Electrochemical methods offer a series of advantages, such as rapid and sensitive response, ease of use and low cost. The development of electrodes for determination of AA in the presence of many interfering species has currently attracted considerable attention in the field of electroanalytical chemistry [10]. Electrochemical methods, especially various amperometric chemical sensors, have been extensively employed for the determination of AA. Various techniques and materials have been employed for the fabrication of chemical sensors including adsorption, cross-linking, layer-by-layer assembly, covalent binding, nanomaterials and so on [11,12].

Carbon nanotubes (CNTs) are widely used in the fabrication of chemical sensors because of their high electrical conductivity, high chemical stability and extremely high mechanical strength [13]. In the last few decades, nanohybrid materials of CNTs with metal or metal oxide nanoparticles have received much attention. Due to their unique properties, these nanohybrid materials have been used in many applications such as chemical sensors, supercapacitor electrodes, catalyst support and antimicrobial therapies. The use of dendrimers as a binder to attach the metal and metal oxide nanoparticles on the surface of CNTs has also been reported [14]. Poly(amido amine) (PAMAM) dendrimers are unimolecular micelles having an amine ($-NH_2$) capped surface which attracts a carboxylic-acid capped pretreated graphite electrode surface ($-COOH$).

In this work, we prepare and characterize a PAMAM dendrimer and AgNPs–MWCNTs composite with poly(neutral red) (PNR)-modified electrode as a working electrode for

the determination of AA. Paraffin wax impregnated graphite electrode (PIGE) was used as a base electrode for this modification. PIGE is also a very useful carbon electrode with low background current, low noise and fast baseline stabilization [15]. The PAMAM/AgNPs–MWCNTs/PNR-modified electrode was studied by using several amperometric methods.

2. Experimental

2.1 *Chemicals and reagents*

Graphite rods (3 mm diameter) were purchased from Aldrich. Ethylenediamine and methyl acrylate were purchased from Merck. AA and neutral red (NR) were obtained from Sisco Research Laboratories, India. Sodium fluoride (NaF) was purchased from Aldrich Chemicals. All the chemicals were of analytical grade and used as such without any further purification. All the supporting electrolytes (0.1 M) and acetate buffer solution (ABS) were prepared with double distilled (DD) water.

2.2 *Apparatus*

The electrochemical experiments were carried out using CHI 400A and CHI 660B electrochemical system (CH instruments, USA). Cyclic voltammetry (CV) was performed using the conventional three-electrode system with the PAMAM/AgNPs–MWCNTs/PNR-modified electrode as the working electrode, a platinum wire as the counter electrode and standard calomel electrode as the reference electrode. The potential window for CV was from –1.0 to 1.0 V and the scan rate was 50 mV s^{-1}. pH of the solution was measured using a digital pH meter (Digisun Electronics System). All experiments were performed at room temperature.

2.3 *Modification of PAMAM/AgNPs–MWCNTs/PNR film-modified electrode*

PAMAM dendrimer was synthesized as reported earlier [16–18]. AgNPs were prepared as previously described [19]. The PIGE was prepared as reported earlier [20]. Graphite electrodes have a number of pores, which are modified when materials are easily absorbed inside the electrodes and become non-reusable. To avoid this condition, molten paraffin wax was used to fill the pores under vacuum conditions. The electrodes were taken out and solidified paraffin on the surface was removed by a knife. The polished circular end of the PIGE was immersed in 0.5 M H_2SO_4 solutions and a potential of 1.6 V was applied for 5 min to promote the carboxylic acid groups on the circular end surface of the PIG electrode. This is called as a pre-treated graphite electrode (PGE). The PGE was immersed in 0.1 M NaF solution containing PAMAM dendrimer (1.6 μM) and electrochemically deposited on the surface of PIGE by applying a potential of 0.6 V for 1 h. The PAMAM-coated electrode was taken out and allowed to dry at room temperature. The AgNPs–MWCNTs nanomaterials composite was prepared with 0.5×10^{-4} M MWCNTs dispersed in 100 μl of ethanol under ultrasonication for 30 min. The MWCNTs (100 μl) dispersion was mixed with 100 μl of AgNPs, and the mixture was kept under ultrasonication for 1 h at room temperature. The MWCNTs nanomaterial composite was drop cast on the PAMAM-coated electrode surface and allowed to dry at room temperature. Then the PAMAM/AgNPs–MWCNTs-modified electrode was dipped in the 0.025 M phosphate buffer solution (PBS) (pH 5.5) + KNO_3 (0.1 M) solution containing 5×10^{-4} M NR. The NR was electropolymerized over the surface of PAMAM/AgNPs–MWCNTs-modified electrode by scanning the potential from –1.0 to 1.0 V for 20 cycles at a scan rate of 50 mV s^{-1}. The resulting PAMAM/AgNPs–MWCNTs/PNR-modified electrode was used for the electrocatalytic oxidation of AA.

3. Results and discussion

3.1 *The polymerization of NR over the PAMAM/AgNPs–MWCNTs-modified electrode*

The electropolymerization of NR on the surface of PAMAM/AgNPs–MWCNTs-modified electrode was carried out by applying the potential of −1.0 to 1.0 V for 20 cycles (figure 1). The NR solution concentration was 5×10^{-4} M in 0.025 M PBS (pH 5.5) + 0.1 M KNO_3. The addition of 0.1 M KNO_3 to the supporting electrolyte was done as the catalytic effect of NO_3^- anions was observed on the electropolymerization of phenazine and phenothiazine dyes [21–25]. The cyclic voltammograms showed two redox couples, the first redox couple around −0.45 and −0.75 V due to the PNR film on PAMAM/AgNPs–MWCNTs-modified electrode and hence an increase in current and the second redox

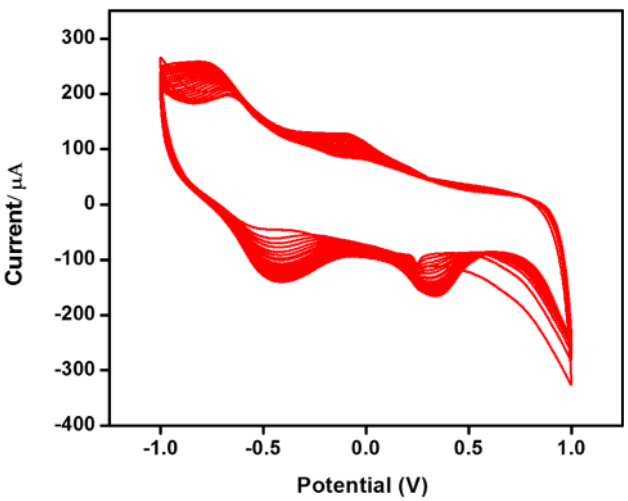

Figure 1. Electrochemical polymerization of NR (5×10^{-4} M) in 0.05 M PBS (pH 5.5) + 1.0 M KNO_3 at a scan rate of 50 mV s^{-1}.

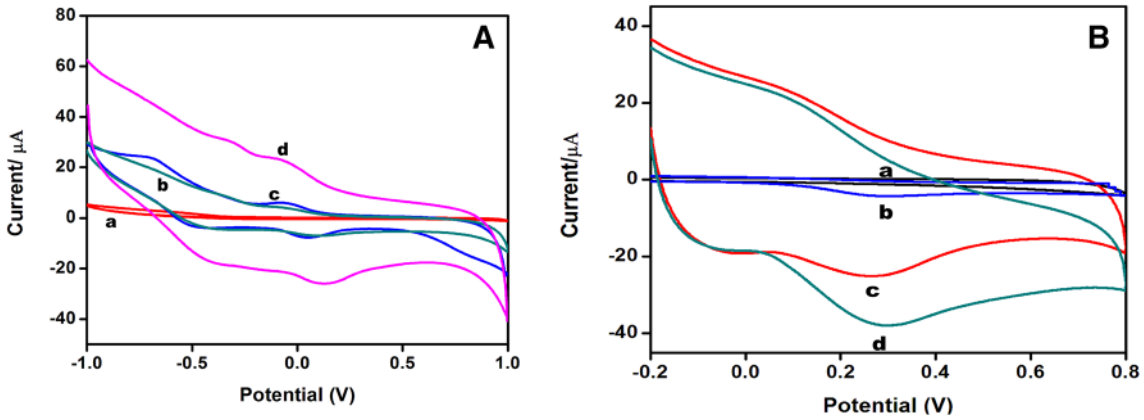

Figure 2. (**A**) CVs of bare PIGE (curve a), PAMAM/AgNPs (curve b), PAMAM/AgNPs/MWCNTs-modified electrode (curve c) and PAMAM/AgNPs/MWCNTs/PNR-modified electrode (curve d) in 0.1 M ABS of pH 4.0 at a scan rate of 50 mV s^{-1}. (**B**) CVs of bare and PAMAM/AgNPs–MWCNT/PNR-modified electrode in the absence (a, c) and in the presence (b, d) of 163 μM of AA in 0.1 M ABS of pH 4.0 at a scan rate of 50 mV s^{-1}.

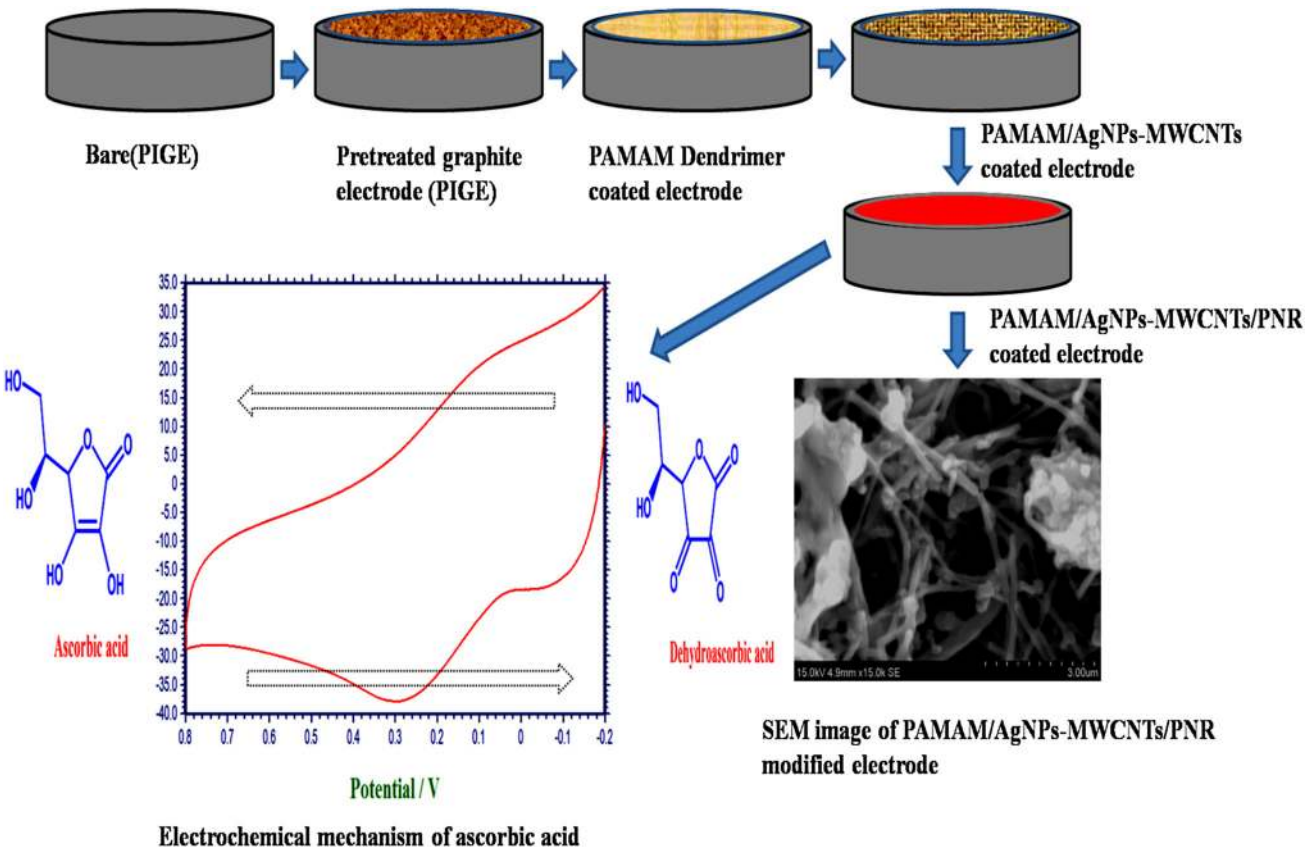

Scheme 1. The illustration of electrode preparation and mechanism of PAMAM/AgNPs–MWCNTs/PNR-modified electrode towards the determination of AA.

couple around 0.33 and −0.09 V corresponding to doping and de-doping of the polymer, increasingly broadening with the number of cycles. The irreversible oxidation peak of NR monomer was observed at 0.9 V [22]. However, in neutral solutions, the oxidized NR released a proton which makes it uncharged and thus slightly soluble. In order to achieve a balance between these opposing tendencies, pH 5.5 was chosen for electropolymerization [23]. The peak current at −0.45 V

increased for successive cycles due to the growth of the PNR films over the surface of PAMAM/AgNPs–MWCNTs-modified electrode. Once the polymer film was formed, the PAMAM/AgNPs–MWCNTs/PNR electrode was dipped in 0.1 M ABS of pH 7 and scanned at a potential range from −1.0 to 1.0 V to confirm the formation of polymer film and stability.

3.2 *Electrochemical behaviour of the PAMAM/AgNPs–MWCNT/PNR-modified electrode*

The cyclic voltammetric investigation of the bare electrode (curve a), PAMAM/AgNPs electrode (curve b), PAMAM/AgNPs/MWCNTs electrode (curve c) and PAMAM/AgNPs/MWCNTs/PNR-modified electrode (curve d) are shown in figure 2A. The PAMAM/AgNPs electrode (curve b), PAMAM/AgNPs/MWCNTs electrode (curve c) showed a very lower current response and the oxidation and reduction peak occurred due to the AgNPs. The cyclic voltammetric response of the bare electrode did not show any characteristic peak (curve a). The electrochemical response of PAMAM/AgNPs–MWCNTs/PNR-modified electrode in the presence of AA was investigated by CV, chronoamperometry (CA), hydro-dynamic voltammetry (HDV) and differential pulse voltammetry (DPV). Figure 2B illustrates the CVs of bare (a) and PAMAM/AgNPs–MWCNT/PNR-modified in the absence (c) and presence (b, d) of 163 μM AA. The bare PIGE oxidized AA at 0.4 V but the PAMAM/AgNPs–MWCNTs/PNR-modified electrode oxidized at a very low potential of around 0.26 V. The PAMAM/AgNPs–MWCNTs/PNR-modified electrode showed an anodic peak (E_{pa}) and cathodic peak (E_{pc}) at 0.26 and 0.07 V respectively, and a formal potential E° [$E^{\circ} = (E_{pa} + E_{pc})/2$] of 0.16 V. The value of ΔE_p was [$\Delta E_p = E_{pa} - E_{pc}$] 0.19 V. Therefore, due to the effect of background electrolyte, pH-modified electrode oxidizes AA at very low potential and the peak current is higher when compared with bare PIGE. This is due to the presence of PNR film incorporated with AgNPs–MWCNTs and PAMAM, which enhances the electrocatalytic activity of the electrode towards the oxidation of AA. Scheme 1 shows a possible mechanism for the electrocatalytic oxidation of PAMAM/AgNPs–MWCNTs/PNR-modified electrode in the presence of AA.

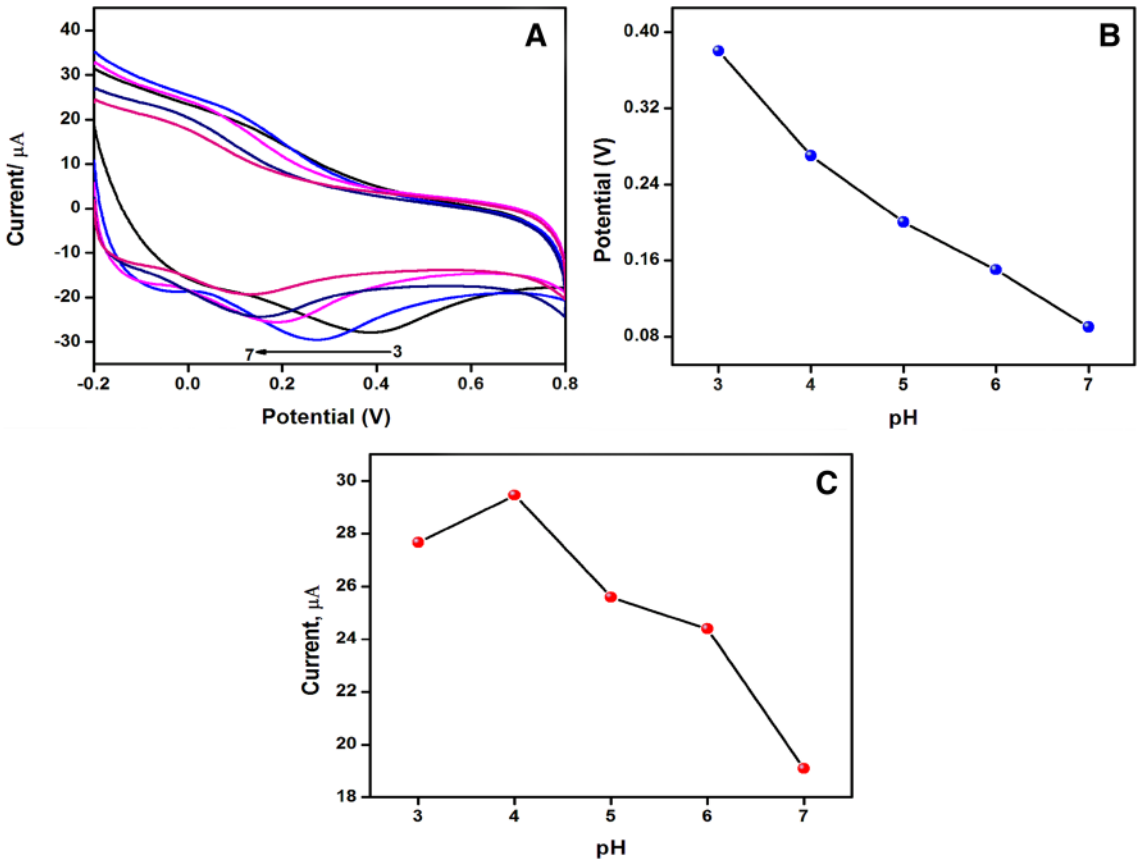

Figure 3. (**A**) Cyclic voltammograms of PAMAM/AgNPs–MWCNTs/PNR-modified electrode containing 81.5 μM AA in ABS at different pH (pH 3–7). (**B**) The calibration plot of potential response *vs*. pH. (**C**) The calibration plot of current response *vs*. pH.

3.3 *Effect of supporting electrolyte and pH*

Cyclic voltammetric methods were carried out to find a favourable supporting electrolyte for the PAMAM/AgNPs–MWCNTs/PNR-modified electrode. The PAMAM/AgNPs–MWCNTs/PNR-modified electrode was scanned between –0.2 and 0.8 V in 0.1 M of various electrolyte solutions such as KNO_3, NaCl, KCl, $NaNO_3$, NaOH, NH_4Cl and ABS. The ABS presents an excellent response towards the redox reactions of PAMAM/AgNPs–MWCNTs/PNR-modified electrode and hence ABS was chosen as the supporting electrolyte for further electrochemical studies. To study the effect of pH of PAMAM/AgNPs–MWCNTs/PNR-modified electrode in the presence of AA (81.5 μM), the pH of ABS was varied from 3 to 7 (figure 3A). The voltammetric results collected from –0.2 to 0.8 V display reversible oxidation and reduction peaks. It is also observed that the peak current decreases as pH increases from 5–7. The influence of pH on the peak current of AA has shown that it reached a maximum at ABS pH 4. Furthermore, the maximum oxidation current may be observed at pH 4.0 because of the effective interaction between PAMAM/AgNPs–MWCNTs/PNR and AA, so pH 4 was chosen as an optimized pH value for the electrochemical determination of AA. When the pH value of electrolyte is > 5, it may affect the sensitivity and conductivity of PAMAM/AgNPs–MWCNTs/PNR at the modified electrode surface. Figure 3B shows the calibration plot of potential response *vs*. pH and figure 3C shows the calibration plot of current response *vs*. pH. The pH *vs*. peak potential corresponding linear equation is $E_{pa}(V) = (0.568 \pm 0.07)x + (0.033 \pm 0.006)$ ($R^2 = 0.978$). The correlation between peak potential and pH is given by the following equation:

$$dE_{pa}/dpH = 2.303mRT/nF \quad (1)$$

where m is the number of protons, n is the number of electrons and F, R and T have their standard meanings. The proportion of the electrons and protons involved in the electrocatalytic oxidation of AA is 1:1. The number of protons involved in the reaction was calculated to be 2. The possible mechanism for the catalytic oxidation is as shown below.

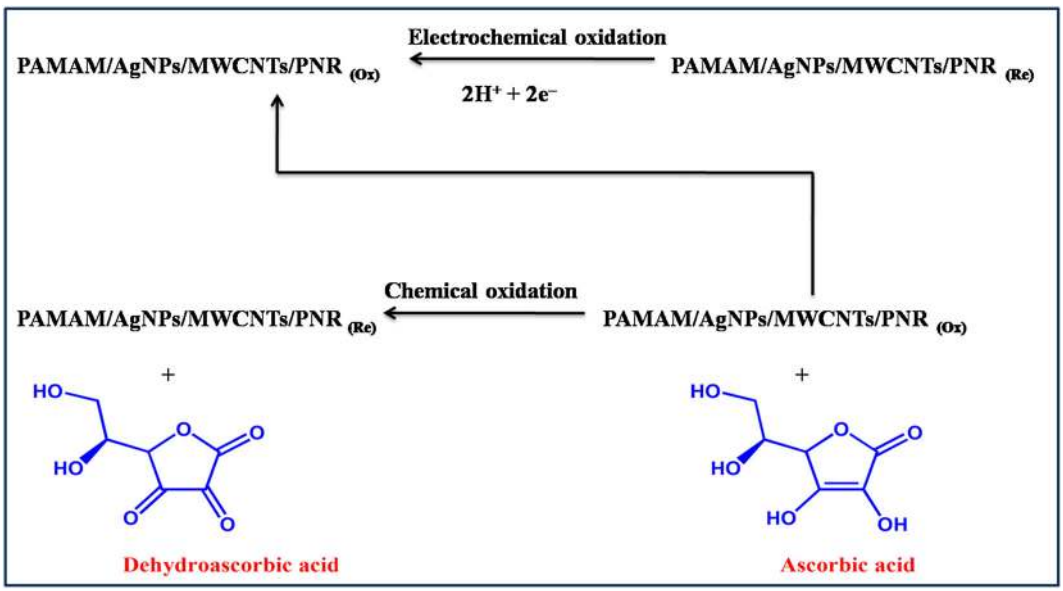

3.3a *Mechanism*: The active surface concentration (Γ) PAMAM/AgNPs–MWCNTs/PNR-modified electrode was calculated by the following equation:

$$\Gamma = \frac{Q}{nFA}. \quad (2)$$

The CVs response of PAMAM/AgNPs/MWCNTs/PNR-modified electrode (curve c) at the scan rate of 50 mV s^{-1} was used to obtain the charge (Q). The obtained values have been substituted in the equation given above, where n is the number of electron transfer ($n = 2$), A is the electrode surface area ($A = 0.07$ cm^2) and F, R and T have their standard meanings. The value of Γ was calculated to be 3.0989×10^{-10} mol cm^{-2}. The redox activity of the PNR on PAMAM/AgNPs/MWCNTs is an electrochemical process that involves two electrons and two protons per site according to the following equation:

$$I_p = \frac{QnFv}{4RT} \quad (3)$$

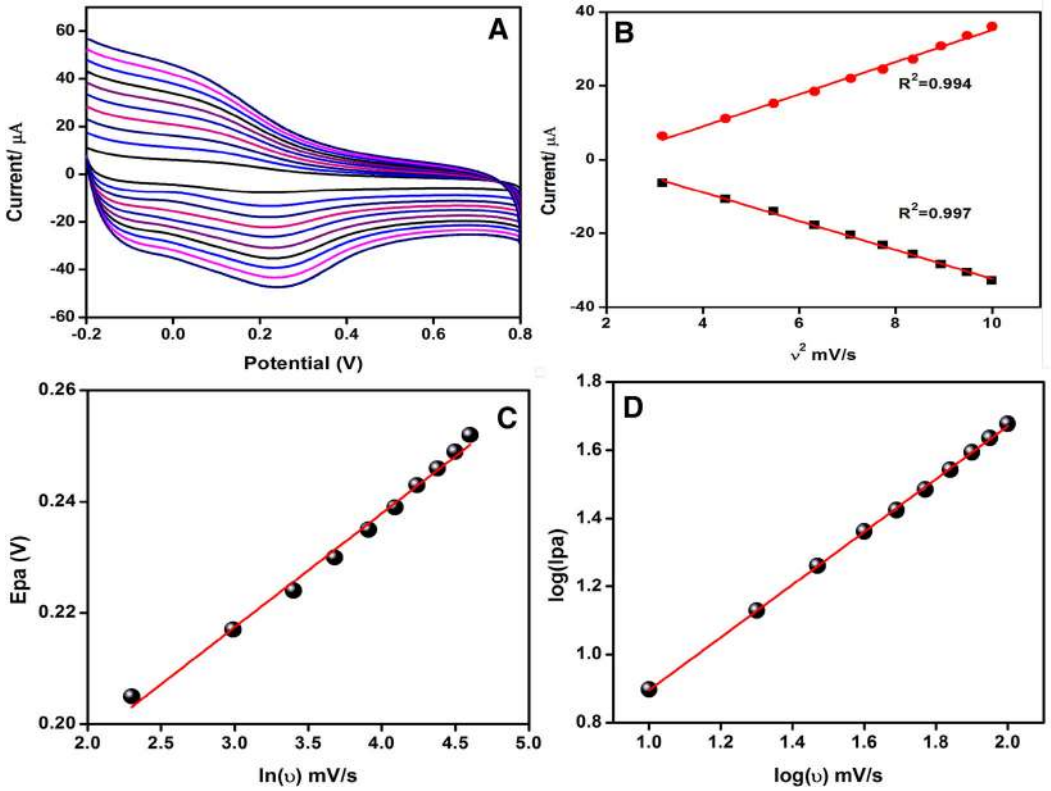

Figure 4. (**A**) Cyclic voltammograms of 81.5 µM AA at PAMAM/AgNPs–MWCNTs/PNR-modified electrode at different scan rates (10, 20, 30, 40, 50, 60, 70, 80, 90 and 100 mV s^{-1}) in 0.1 M ABS of pH 4.0. (**B**) Relationship between anodic peak current, cathodic peak current and square root of scan rate. (**C**) Relationship between anodic peak potential and ln scan rate. (**D**) Relationship between logarithmic anodic peak current and logarithmic scan rate.

where I_p = peak current (µA), A = surface area of the electrode (cm^2) and ν = scan rate (mV s^{-1}). F, R and T have their standard meanings.

3.4 *Effect of scan rate*

In order to study the nature of the electrode process at the PAMAM/AgNPs–MWCNTs/PNR-modified electrode surface, CVs were recorded at different scan rates. Figure 4A shows the CVs corresponding to 81.5 µM AA using PAMAM/AgNPs–MWCNTs/PNR-modified electrode at different scan rates (10, 20, 30, 40, 50, 60, 70, 80, 90 and 100 mV s^{-1}) in 0.1 M ABS of pH 4.0. It has been observed that the oxidation and reduction peak current increased linearly with increase in scan rate. Figure 4B illustrates the relationship between anodic peak current, cathodic peak current *vs.* square root of scan rate. The I_{pa} and I_{pc} increased linearly with ($\nu^{1/2}$), and the corresponding regression equation was $I_{pa} = (6.707 \pm 3.903)x + (0.46 \pm 0.06)$ ($R^2 = 0.997$) and $I_{pc} = (-8.366 \pm 4.348)x + (0.82 \pm 0.11)$ ($R^2 = 0.994$) for anodic and cathodic scans respectively. Figure 4C and D illustrates the relationship between anodic peak potential (E_{pa}) *vs.* ln scan rate (ln ν) and log anodic peak current (log I_{pa}) *vs.* log scan rate (log ν) respectively. Figure 4C shows E_{pa} increased linearly with (ln ν), and the corresponding regression equation was E_{pa} (V) $= (0.155 \pm 0.020)x + (0.002 \pm 6.013)$ ($R^2 = 0.9923$). The relationship between E_{pa} *vs.* log(ν) for analytical oxidation peak is studied and observed that, as the scan rate increases, the peak potential shifts to a more positive value. A linear relationship is observed in the range 10–100 mV s^{-1}. A linear relationship is observed between log I_{pa} and log ν and the corresponding equations and correlation coefficients are expressed for $I_{pa} = (0.120 \pm 0.775)x + (0.008 \pm 0.005)$ ($R^2 = 0.9996$). Figure 4D shows a double logarithmic plot of log(ν) *vs.* log(I_{pa}), from which the slope value was found to be 0.77 resembling an electron transfer process that is adsorption controlled. The relationship between ln(ν) and E_{pa} (V) can be expressed as Laviron equation [26]:

$$E_{pa} = E^{\circ} - \frac{RT}{(1-\alpha)nF} \ln \frac{RTK_s}{(1-\alpha)nF} + \frac{RT}{(1-\alpha)nF} \ln \nu \quad (4)$$

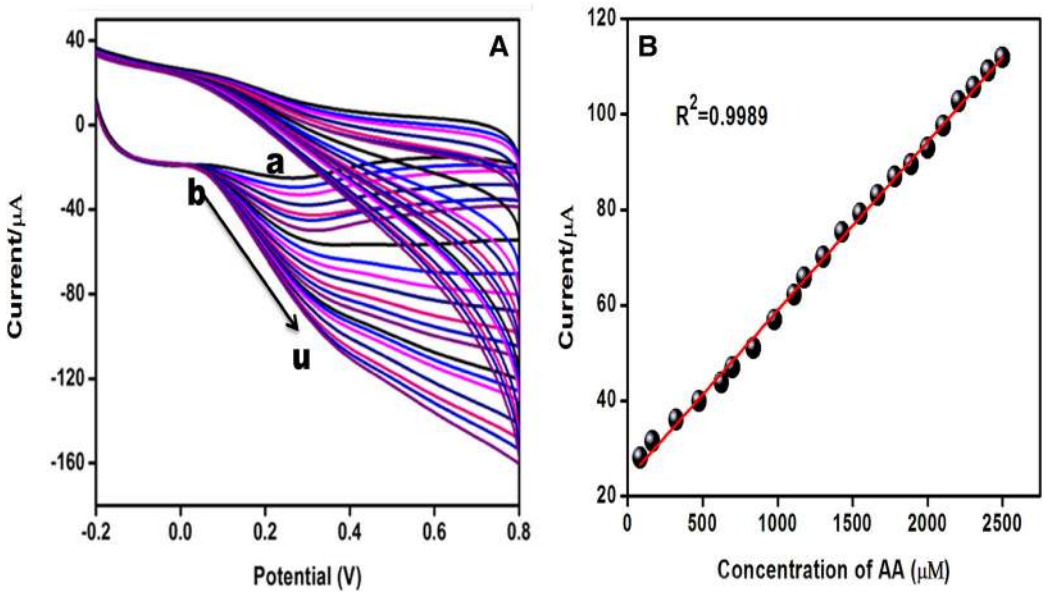

Figure 5. (**A**) CV response of PAMAM/AgNPs–MWCNT/PNR-modified electrode in the absence (a) and in the presence (b–u) of successive additions of AA (81.5 to 2500 μM) in 0.1 M ABS of pH 4 at the scan rate of 50 mV s^{-1}. (**B**) The calibration plot of current response *vs*. concentration of AA.

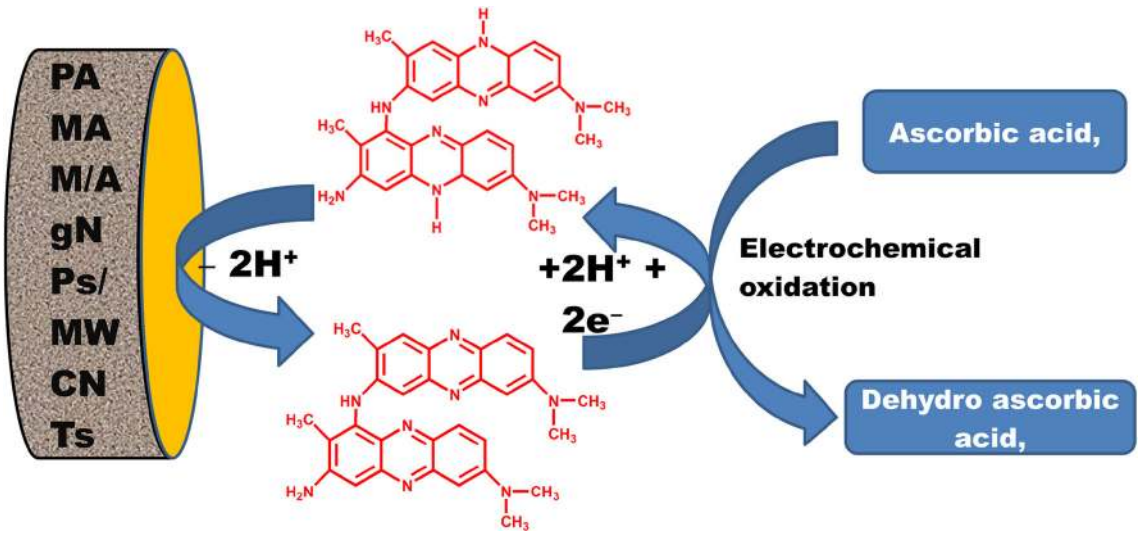

Scheme 2. PAMAM/AgNPs−MWCNTs/PNR-modified electrode electrocatalytic oxidation with AA.

where α is the charge transfer coefficient; v is the scan rate in mV s^{-1}; n is the number of electrons transferred; K_s is the electron transfer rate constant; and R, T and F have their standard meanings [27]. The value of α=0.61 was calculated from the slope of log(v) *vs*. log(I_{pa}) which indicates a reversible electrode process. Substituting the Laviron equation, the K_s for the electrochemical reaction involving PAMAM/AgNPs–MWCNTs/PNR-modified electrode was calculated to be 0.17 s^{-1}.

3.5 *Electrochemical oxidation of AA by PAMAM/AgNPs–MWCNT/PNR-modified electrode*

Figure 5A shows the CVs responses of PAMAM/AgNPs–MWCNTs/PNR-modified electrode on different concentrations of AA. Curves b to u represent the presence of AA from 81.5 to 2500 μM at the potential ranging from −0.2 to 0.8 V in 0.1 M ABS of pH 4 at a scan rate of 50 mV s^{-1}. Figure 5B shows the calibration plot of current

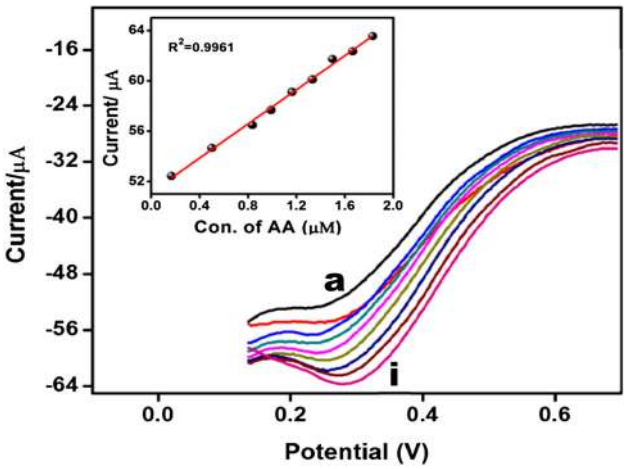

Figure 6. DPV response of PAMAM/AgNPs–MWCNT/PNR-modified electrode in the presence (a–i) of successive additions of AA (0.16–1.6 μM) in 0.1 M ABS of pH 4 at the scan rate of 50 mV s^{-1}. The insert shows the calibration plot of current response *vs.* concentration of AA in the range of 0.16–1.6 μM.

response *vs*. concentration of AA. By increasing the concentration of AA, the oxidation current also increased linearly and a correlation coefficient was 0.9989. Scheme 2 shows the redox features of the PAMAM/AgNPs–MWCNTs/PNR-modified electrode.

3.6 *Differential pulse voltammetry*

In order to improve the sensitivity for the electrocatalytic oxidation of AA, DPV has been employed to record the oxidation current of the PAMAM/AgNPs–MWCNTs/PNR-modified electrode. Figure 6 shows the DPV measurements of PAMAM/AgNPs–MWCNTs/PNR-modified electrode in the presence of different concentrations of AA in ABS (pH 4.0). The DPV response of the AA increased with increasing concentration. A linear relationship was obtained between the peak currents and the concentration of AA over the range from 0.16 to 1.6 μM (inset). The corresponding linear regression equation is I_{pa} (μA) = $(0.317 \pm 0.061)x + (8.957 \pm 8.548)$ (R^2 = 0.9961). The limit of detection of AA was determined to be 0.053 μM. These results clearly indicate that PAMAM/AgNPs–MWCNTs/PNR-modified electrode has excellent capacity for the determination of AA. The proposed method is compared with already reported methods and the comparative results are shown in table 1.

3.7 *Determination of AA under dynamic conditions*

The applicability of PAMAM/AgNPs–MWCNTs/PNR-modified electrode for determination of AA in the flow system was evaluated by performing hydrodynamic voltammogram studies. Figure 7 shows the hydrodynamic voltammograms of bare PIG electrode (a) and PAMAM/AgNPs–MWCNTs/PNR-modified electrode (b) in the presence of 81.5 μM AA (curve a and b respectively) in ABS of pH 4 at a scan rate of 50 mV s^{-1} under stirring rate of 300 rpm. The results of hydrodynamic voltammogram studies showed a good response of PAMAM/AgNPs–MWCNTs/PNR-modified electrode at 0.25 V (curve b). The results indicated the fact that the electrocatalytic oxidation of AA by the PAMAM/AgNPs–MWCNTs/PNR-modified electrode was favoured even in the dynamic conditions. The hydrodynamic voltammogram studies of the bare PIG electrode (curve a) did not show any considerable current response compared to the PAMAM/AgNPs–MWCNTs/PNR-modified electrode (curve b) under similar conditions.

Table 1. Comparison of electrochemical detection of AA using different types of modified electrodes.

Electrode	Electrolyte pH	Technique	Linear range (μmol l^{-1})	LOD (μmol l^{-1})	Reference
Pd-CNFs/CPE	0.1 M PBS pH 4.5	DPV	50–4000	15	[28]
ERGO/GCE	0.1 M PBS pH 7.0	DPV	500–2000	250	[29]
Pd_3 Pt1/PDDA–RGO	0.1 M PBS pH 7.4	DPV	40–1200	0.61	[30]
Au@Pd–RGO/GCE	0.1 M PBS pH 7.0	DPV	0.1–1000	0.02	[31]
Chitosan–graphene GCE	0.05 M PBS pH 7.0	DPV	50–1200	50	[32]
PTCA/PDAox/GC	0.1 M PBS pH 3.0	DPV	76–3900	25.3	[33]
P-4-ABA/GCE	0.2 M PBS pH 4.5	DPV	20–800	5.0	[34]
Poly(Tyr)/MWCNTs–COOH/GCE	0.067 M PBS pH 7.4	DPV	50–1000	2.0	[35]
CPE/MWCNTs/IL/PdNPs	0.1 M PBS pH 5.0	DPV	0.6–112	0.200	[36]
PAMAM/AgNps	0.1 M PBS pH 4.0	DPV	17–1428	5.5	This work
PAMAM/AgNPs–MWCNTs	0.1 M PBS pH 4.0	DPV	8–1895	2.8	This work
PAMAM/AgNPs–MWCNTs/PNR	0.1 M PBS pH 4.0	DPV	0.2–2500	0.053	This work

Pd-CNFs/CPE: palladium nanoparticle-loaded carbon nanofibres, GCE: glassy carbon electrode, ERGO: reduced graphene oxide, Pd_3 Pt1/PDDA–RGO: graphene anchored with Pd–Pt nanoparticles, Au@Pd-RGO: Au@Pd-reduced graphene oxide nanocomposites, PTCA/PDAox/GC: 3,4,9,10-perylenetetracarboxylic acid/oxidized dopamine polymer, P-4-ABA/GCE: poly(4-aminobutyric acid)-modified glassy carbon electrode, CPE/MWCNTs/IL/PdNPs: carbon paste electrode/multi-walled CNTs/ionic liquid/palladium nanoparticles.

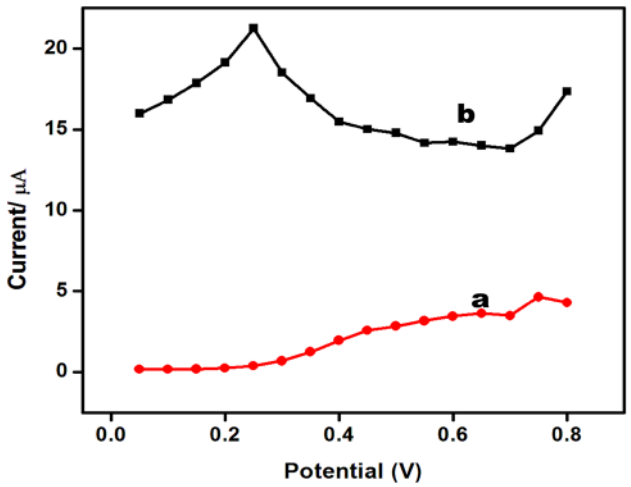

Figure 7. Hydrodynamic voltammograms of the bare (a) and PAMAM/AgNPs–MWCNTs/PNR-modified electrode (b), 0.1 M ABS of pH 4.0, in the presence of 81.5 μM AA at a scan rate of 50 mV s^{-1} under stirring conditions.

3.8 *The amperometric response of the PAMAM/AgNPs–MWCNTs/PNR-modified electrode*

The PAMAM/AgNPs–MWCNTs/PNR-modified electrode has excellent and strong mediating properties and facilitates the low potential amperometric sensor for the determination of AA. Figure 8A shows the chronoamperometric response of AA and the oxidation of AA by PAMAM/AgNPs–MWCNTs/PNR-modified electrode at a fixed potential of 0.25 V was studied under stirring at 300 rpm in ABS of pH 4. The PAMAM/AgNPs–MWCNTs/PNR-modified electrode showed a stepwise increase in the catalytic current with successive addition of AA in the concentration range of 3.32 to 32.25 μM. Figure 8B shows the calibration plot with a linear relationship between catalytic current and concentration of AA in a linear range of 3.32 to 32.25 μM with a correlation coefficient of 0.9958.

3.9 *Reproducibility and interference tests*

PAMAM/AgNPs–MWCNTs/PNR-modified electrode towards AA in the presence of interfering analytes such as gallic acid (GA), L-Tryptophan (L-Try), riboflavin (RF) and butylated hydroxyanisole (BHA) was studied. Amperometric response to the detection of AA at PAMAM/AgNPs–MWCNTs/PNR-modified electrode in the presence of above-mentioned interference in ABS of pH 4 was also observed. The interference was selected based upon their presence in various commercial samples. The effect of the possible interfering substances on the response of the sensor was evaluated at the fixed potential of 0.25 V. Figure 9 shows that the first three additions of 15 μM of AA showed a gradual increase, but the fourth addition of each 60 μM (1:4 ratio) of GA, L-Try, RF and BHA solution caused no significant interference in the response of the sensor. This result showed that the PAMAM/AgNPs–MWCNTs/PNR-modified electrode was highly selective towards the oxidation of AA.

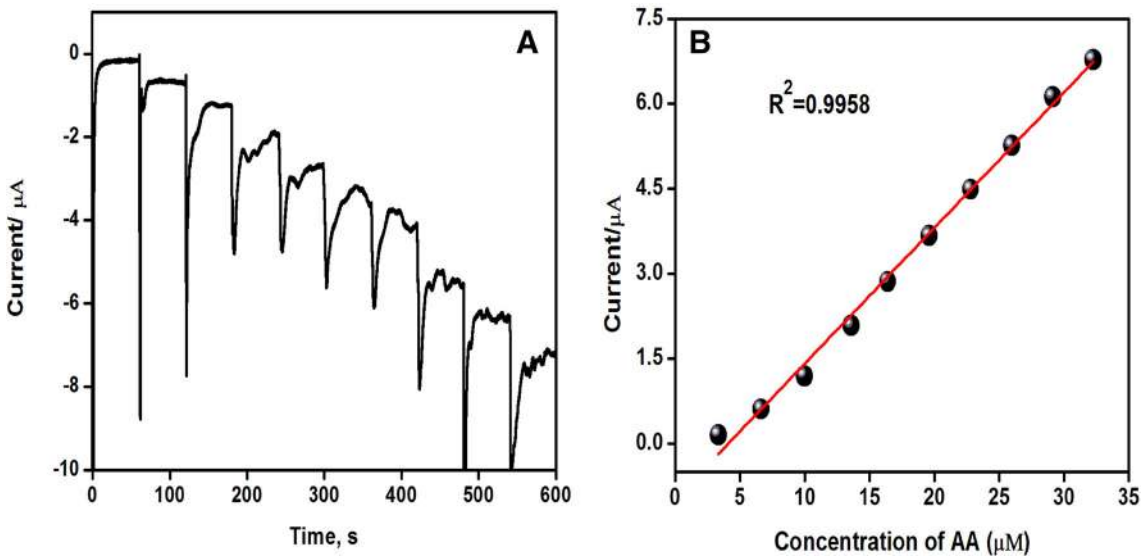

Figure 8. (**A**) Chronoamperometric responses of the PAMAM/AgNPs–MWCNTs/PNR-modified electrode for the successive additions of 0.2 ml of 0.001 M stock solution of AA in 60 ml of 0.1 M ABS of pH 4, at a scan rate of 50 mV s^{-1}, and the applied potential of 0.25 V with a stirring rate of 300 rpm. (**B**) The corresponding calibration plot in the range of 3.32–32.25 μM.

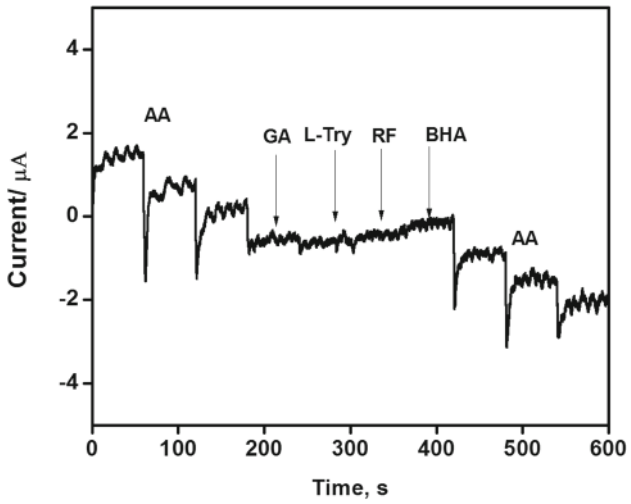

Figure 9. Amperometric response of the PAMAM/AgNPs–MWCNTs/PNR-modified electrode towards interference effect in the determination of AA in the presence of various interferents in 0.1 M ABS of pH 4.0 at a peak potential of 0.25 V with a stirring rate of 300 rpm.

3.10 *Long time stability of the PAMAM/AgNPs–MWCNTs/PNR-modified electrode for AA determination*

In order to assess shelf life of PAMAM/AgNPs–MWCNTs/PNR-modified electrode response at an interval of 5 days towards 81.5 μM AA studies for a period of 60 days showed that the proposed modified electrode retained 94% response at the end (figure 10A). The operating long-time stability of PAMAM/AgNPs–MWCNTs/PNR-modified electrode was analysed by injecting 81.5 μM AA every 30 min over an extended period of 7 h (figure 10B). There is no significant change observed during this period. The above results indicate that the PAMAM/AgNPs–MWCNTs/PNR-modified electrode has both good storage capacity and operational stability as an amperometric sensor.

3.11 *Analysis of pharmaceutical and fruit samples*

The analytical application of the PAMAM/AgNPs–MWCNTs/PNR-modified electrode for the determination of AA was analysed by measuring the concentration of AA in commercially available tablets and fruit samples (lemon and orange juices). The vitamin C tablet powder samples were diluted with DD water and two different volumes of each sample were added to 50 ml of ABS (pH 4.0). Before the test, the fruit juice samples were diluted with 0.1 M ABS (pH 4.0) at an appropriate volume ratio. DPV was employed for the determination of AA. The evaluation of the AA concentration is carried out using a standard addition method. The recovery and relative standard deviation (RSD) values have been tabulated from the analysis (table 2). The results illustrate that the PAMAM/AgNPs–MWCNTs/PNR-modified electrode can be utilized for the real sample analysis.

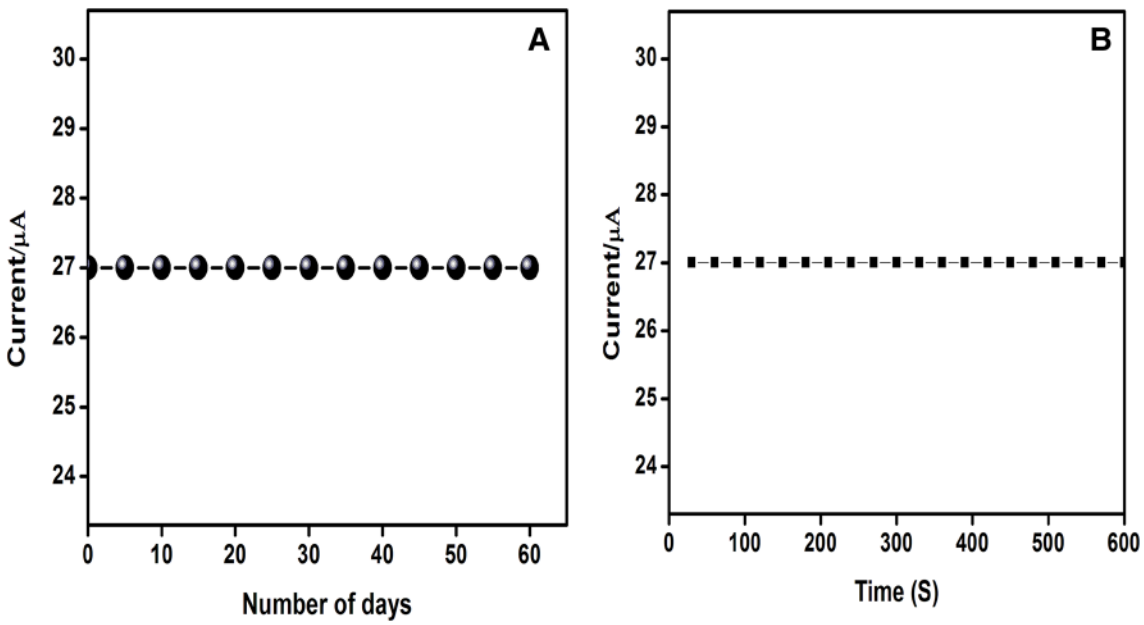

Figure 10. (**A**) Long time stability response of the PAMAM/AgNPs–MWCNTs/PNR-modified electrode towards the oxidation of AA (81.6 μM). (**B**) Current response of the PAMAM/AgNPs–MWCNTs/PNR-modified electrode for AA (81.6 μM) various times.

Table 2. Determination of AA in vitamin C tablets and fruit juices.

Samples	Added (μM)	Found (μM)	RSD (%)	Recovery (%)
Vitamin C tablets				
1	5	5.32 (±0.04)	0.891	106.4
2	10	10.16 (±0.11)	0.873	101.6
Fruit juices				
Lemon	10	10.08 (±0.09)	1.07	100.8
Orange	20	20.10 (±0.03)	0.98	100.5

Source: Average three repeated measurements (±standard deviation).

4. Conclusions

A highly stable PAMAM/AgNPs–MWCNTs/PNR film-modified electrode was fabricated successfully by electropolymerization of NR over PAMAM/AgNPs–MWCNTs electrode. The resulting PAMAM/AgNPs–MWCNTs/PNR-modified electrode was characterized by scanning electron microscopy and CV. Furthermore, the PAMAM/AgNPs–MWCNTs/PNR-modified electrode was investigated for use in the electrocatalytic oxidation of AA. The PAMAM/AgNPs–MWCNTs/PNR-modified electrode was found to be highly stable, selective and sensitive towards the determination of AA. The proposed PAMAM/MWCNTs–AgNPs/PNR film-modified electrode has shown a high determination range of 0.16 to 2500 μM. The PAMAM/AgNPs–MWCNTs/PNR-modified electrode is also used for AA determination in real samples.

Acknowledgements

The authors gratefully acknowledge the DST-Inspire fellowship from the Department of Science and Technology, New Delhi, India for financial assistance.

References

[1] Wang X, Wu P, Hou X and Lv Y 2013 *Analyst* **138** 229
[2] Wu G H, Wu Y F, Liu X W, Rong M C, Chen X and Chen X 2012 *Anal. Chim. Acta* **745** 33
[3] Luo X L, Xu J J, Zhao W and Chen H Y 2004 *Anal. Chim. Acta* **512** 57
[4] Andreu Y, Marcos S, Castillo J R and Galban J 2005 *Talanta* **65** 1045
[5] Anastos N, Barnett N W, Hindson B J, Lenehan C E and Lewis S W 2004 *Talanta* **64** 130
[6] Nováková L, Solichová D and Solich P 2009 *J. Chromatogr. A* **1216** 4574
[7] Suntornsuk L, Gritsanapun W, Nilkamhank S and Paochom A 2002 *J. Pharm. Biomed. Anal.* **28** 849
[8] Saari N B, Osman A, Selamat J and Fujita S 1999 *Food Chem.* **66** 57
[9] Qiu S, Gao S, Liu Q, Lin Z, Qiu B and Chen G 2011 *Biosens. Bioelectron.* **26** 4326
[10] Chairam S, Sriraksa W, Amatatongchai M and Somsook E 2011 *Sensors* **11** 10166
[11] Senel M and Çevik E 2012 *Curr. Appl. Phys.* **12** 1158
[12] Durst R A, Baumner A J, Murray R W, Buck R P and Andrieux C P 1997 *Pure Appl. Chem.* **69** 1317
[13] Ran X Q, Yuan R, Chai Y Q, Hong C L and Qian X Q 2010 *Colloids Surf. B Biointerfaces* **79** 421
[14] Lopez J A, Manrıquez J, Mendoza S and Godınez L A 2007 *Electrochem. Commun.* **9** 2133
[15] Jeykumari S, Ramaprabhu S and Sriman Narayanan S 2007 *Carbon* **45** 1340
[16] Torigoe K, Suzuki A and Esumi K 2001 *J. Colloid Interface Sci.* **241** 346
[17] Ramírez-Segovia A S, Banda-Alemán J A, Gutiérrez-Granados S, Rodríguez A, Rodríguez F J, Godínez A *et al* 2014 *Anal. Chim. Acta* **812** 18
[18] Zhang Y, Ying Xu M and Kun Jiang T 2014 *Chin. Chem. Lett.* **25** 815
[19] Lee S H, Teng C C, Ma C C and Wang I 2011 *J. Colloid Interface Sci.* **364** 1
[20] Cui H, Zou G Z and Lin X Q 2003 *Anal. Chem.* **75** 324
[21] Scholz F and Lange B 1992 *Tr. Anal. Chem.* **11** 359
[22] Yang C M, Yi J L, Tang X J, Zhou G Z and Zeng Y 2006 *React. Funct. Polym.* **66** 1336
[23] Ghica M E and Brett C M A 2006 *Electroanalysis* **18** 748
[24] Yogeswaran U and Chen S M 2007 *Electrochim. Acta* **52** 5985
[25] Carvalho R C, Caridade C G and Brett C M A 2010 *Anal. Bioanal. Chem.* **398** 1675
[26] Purushothama H T and Arthoba Nayaka Y 2017 *Sens. Bio-Sens. Res.* **16** 12
[27] Manjunatha P, Nayaka Y A, Chethana B K, Vidyasagar C C and Yathisha R O 2018 *Sens. Bio-Sens. Res.* **17** 7
[28] Huang J S, Liu Y, Hou H Q and You T Y 2008 *Biosens. Bioelectron.* **24** 632
[29] Yang L, Liu D, Huang J and You T 2014 *Sens. Actuators B* **193** 166
[30] Yan J, Liu S, Zhang Z, He G, Zhou P and Liang H 2013 *Colloids Surf. B Biointerfaces* **111** 392
[31] Jiang J and Du X 2014 *Nanoscale* **6** 11303
[32] Han D, Han T, Shan C, Ivaska A and Niu L 2010 *Electroanalysis* **22** 2001
[33] Liu X, Ou X, Lu Q, Zhang J, Chen S and Wei S 2014 *RSC Adv.* **4** 42632
[34] Zheng X, Zhou X, Ji X, Lin R and Lin W 2013 *Sens. Actuators B Chem.* **178** 359
[35] Li S J, Qian C, Wang K, Hua B Y, Wang F B, Sheng Z H *et al* 2012 *Sens. Actuators B* **174** 441
[36] Rafati A A, Afraz A, Hajian A and Assari P 2014 *Microchim. Acta* **181** 1999